Parameter identification and state estimation of a microalgae dynamical model in sulphur deprived conditions: Global sensitivity analysis, optimization criterion, extended Kalman filter

Moemen Daboussy, Mariana Titica, Lionel Boillereaux

Parameter Identification and State Estimation of a Microalgae Dynamical Model in Sulphur Deprived Conditions: Global Sensitivity Analysis, Optimization Criterion, Extended Kalman Filter

Moemen Daboussy,[1]* Mariana Titica[2] and Lionel Boillereaux[2]

1. Université de Bourgogne, DRIVE, EA 1859, ISAT, 49, rue Mademoiselle Bourgeois, BP 31 58027, Nevers Cedex, France

2. Université de Nantes, GEPEA, UMR CNRS 6144, CRTT, Boulevard de l'Université, BP 406 F-44602, Saint-Nazaire Cedex, France

In this article, a dynamic model describing the growth of the green microalgae *Chlamydomonas reinhardtii*, under light attenuation and sulphur-deprived conditions leading to hydrogen production in a photobioreactor is presented. The strong interactions between biological and physical phenomena require complex mathematical expressions with an important number of parameters. This article presents a global identification procedure in three steps using data from batch experiments. First, it includes the application of a sensitivity function analysis, which allows one to determine the parameters having the greatest influence on model outputs. Secondly, the most influential parameters were identified by using the classical least-squares cost function. This stage is applied to the experimental data collected from a lab-scale batch photobioreactor. Finally, the implementation of an Extended Kalman Filter estimating the biomass concentration, extracellular and intracellular sulphur concentrations is presented. Thereby, the observer uses on-line measurements provided by a mass spectrometer measuring the outlet gas composition (O_2, CO_2). Software sensor performances and limits are illustrated in simulation and with experimental data.

Keywords: sensitivity function, cost function, extended Kalman filter, photobioreactor, *Chlamydomonas reinhardtii*

INTRODUCTION

The world is in desperate need of a novel source of sustainable and renewable energy, without greenhouse gas emissions or environmental pollution. Photoautotrophic H_2 produced from solar energy by microalgae might be this energy. This process produces H_2 and O_2, and consumes CO_2. For inducing H_2 production in a photobioreactor, anaerobic conditions are required, as well as sulphur deprivation conditions.[1]

To optimize the process, both modelling and experimentations at a laboratory scale in controlled conditions are required. As a first approach, phenomenological models based on mass balance equations coupled with kinetic expressions are used in general. Photosynthetic growth can also be formulated as a function of the amount of sulphur accumulated in cells. This is achieved by incorporating an intracellular quota formulation based on the Droop model.[2] The later model is classically used in oceanographic studies[3] to consider the relation of microalgal growth to the nutrient availability. In the case of light-limited growth culture in a photobioreactor, as presented here, this formulation has to be associated with radiative transfer conditions, introducing the coupling between a radiative model[4] and a Haldane model to represent light-dependent photosynthetic growth kinetics.

The strong interactions between biological and physical phenomena lead to complex mathematical expressions with an important number of parameters that have to be identified using the available experimental data. Parameter identification becomes a difficult task because of the complexity of models as well as the lack of sufficient and reliable experimental data. Several works are reported in literature that deal with questions of structural and practical identifiability of bioprocess models, as well as experiment design for its identification, and suitable methods to carry out this identification.[5] Sensitivity analysis appears as a powerful tool to determine the parameters that have the biggest influence on model outputs, while avoiding over-parameterization and reducing the complexity of the model, as discussed by Bastin and Dochain.[6] Sensitivity analysis has recently been applied to biological models such as plant cell cultures.[7] Moreover, the shape of the sensitivity function as a function of time allows for choosing the time range during which the identification of a parameter can be the most accurate. In fact, the higher the amplitude of a sensitivity function during a certain time period, the more the parameter identification will be accurate in this time interval.

A key role in the success of an identification procedure is held by the computation of the sensitivity of the measured outputs with regard to the model parameters, as well as an appropriation of the cost function, which measures the deviation between the model and measured outputs. Moreover, the proper application of an optimization procedure may be important. Several cost functions have been used for kinetic parameter estimation, following an output-error criterion. The type of function that is selected may influence how the optimization proceeds, adjusting one or another parameter.[8]

The accessibility to process measurements and to culture physiological states is limited. Therefore, in this context, we developed a software sensor for on-line estimating of key parameters contributing to hydrogen production. The work is based on a dynamic model describing the evolution of extra- and intracellular sulphur, total biomass and intracellular starch concentrations as a

*Author to whom correspondence may be addressed.
E-mail address: moemendaboussy@hotmail.com
Can. J. Chem. Eng. 92:1378–1395, 2014

function of environmental conditions. This model is analyzed in order to elaborate on estimation strategies at the photobioreactor level. Many studies have been made on the state estimation of unmeasured states variables, among others several estimation techniques have been proposed in the literature.[9–10]

In this article, the sensitivity analysis and optimization procedure are applied on a dynamic model describing the growth of the green microalgae *Chlamydomonas reinhardtii*, under light attenuation and sulphur deprived conditions leading to hydrogen production in a photobioreactor. A Droop formulation was used to describe the evolution of extra- and intracellular sulphur, as a function of environmental conditions.[1] We present also the development of an extended Kalman filter (EKF) using on-line measurements of gas composition at the photobioreactor outlet as an indirect measurement of the biomass concentration.

The article is organized as follows: the "Methods" section presents the method used to describe the dynamic process model, as well as parameter identification, and the implementation of EKF. The results of application are shown in the "Results and Discussions" section. Finally, conclusions are given in the end section.

METHODS

Process Description

Photobiological H_2 production by green microalgae is a transitory phenomenon, taking place under anoxic conditions and in the presence of illumination. The main limitation in the H_2 production is the inhibition of its production by the oxygen. As soon as oxygen is released during water photolysis by photosynthesis, H_2 release stops. Anoxic conditions into the cultivation systems could be induced in sulphur deprivation conditions.[1]

The H_2 production in batch mode could be represented by a succession of three stages:

- *Photosynthetic growth phase*, during which the microalgae is growing, assimilating CO_2 and nutrients (N, P, S), in the presence of illumination. During this phase, O_2 is released; biomass concentration increases, progressively inducing light limitation phenomena. The initial amount of sulphur introduced into the cultivation system has to be determined in order to achieve its total consumption (deprivation).
- *Sulphur deprivation phase*: Once the total consumption of extracellular S is achieved, O_2 release decreases progressively resulting in a transition to anoxia. Intracellular sulphur concentration accumulated during the first phase is progressively consumed.
- *H_2 production phase*–when anoxic conditions are obtained. The H_2 production is accompanied with intracellular starch consumption.

The model analyzed here describes the transition from the first to the second phase (photosynthetic and sulphur deprivation). The evolutions of extra- and intracellular sulphur concentrations and biomass concentration during these phases are described by a set of three mass balance equations, as presented hereafter.

Dynamic Process Model

Let us first consider a continuous-time state-space model described by the following nonlinear differential equations:

$$\begin{cases} \dot{x} = f(x) + \sum_{i=1}^{m} g_i(x)u_i \\ y_i = h_j(x) \text{ with } j = 1, \ldots, m \end{cases} \quad (1)$$

where $x \in R^n$ is the state vector, $u \in R^m$ is the vector of inputs, $y \in R^m$ is the vector of outputs, $f(x)$ is an n-dimensional vector of nonlinear functions, $g(x)$ is an $(n \times m)$-dimensional matrix of nonlinear functions, and $h(x)$ is an m-dimensional vector of nonlinear functions.

In our case, the state vector of the system consists of three variables $x = (X, S, Q)$ which are, respectively, the biomass concentration (X), the extracellular-sulphur concentration (S), and intracellular sulphur quota (Q) (expressed as intracellular sulphur concentration divided by the biomass concentration). The input vector consists of two variables, the incident light intensity and dilution rate $u = (Io, D)$ which can be used as control variables.[11]

The model equations consist of mass balance equations at the photobioreactor level, assuming perfectly stirred conditions. Two kinetic rates were used for describing biological phenomena, namely the specific growth rate, depending on available light and on the internal sulphur quota, and an absorption rate of the extracellular sulphur into the cell, providing the internal sulphur quota.

The mass balance equations are:

$$\frac{dX}{dt} = (f_Q) < \mu_G > X - \mu_s X - DX \quad (2)$$

$$\frac{dS}{dt} = -Y_{sx}\left(< \mu_G > \frac{S}{S + k_s} \right) X + D(S_i - S) \quad (3)$$

$$\frac{dQ}{dt} = Y_{sx} < \mu_G > \frac{S}{S + k_s} - (f_Q) < \mu_G > Q \quad (4)$$

where D represents the dilution rate (h^{-1}) (expressed as the feeding flow divided by the reactor volume, $D = 0$ in batch mode), and S_i represents the sulphur concentration in the feeding flow.

The growth rate dependency on light is given by:

$$\mu_G = \mu_{max} \frac{G_z}{K_I + G_z}$$

where μ_{max} is the maximal specific growth rate (h^{-1}), G_z is the irradiance inside the culture (mol photon^{-2} s^{-1}), and K_I is the half-saturation constant (mol photon^{-2} s^{-1}).

Compared with the original model of Fouchard et al.[1] a simplified formula[12] was used for describing the local value of irradiance G_z within the culture medium:

$$\frac{G_z}{I_0} \cong \exp\left[-\frac{(1+\alpha)}{2\alpha} E_a X z \right]. \quad (6)$$

In this formula, I_0 is the incident light intensity, α is the module of linear diffusion, and E_a is the mass coefficient of absorption of radiation. z is the culture depth, as light attenuation occurs along only one direction, namely, the depth of culture z, perpendicular to the illuminated surface. The average photosynthetic rate $<\mu_G>$ calculated all over the reactor volume is obtained by integrating local photosynthetic responses as follows:

$$< \mu_G > = \frac{1}{L} \int_0^L \mu_G(G(z)) dz. \quad (7)$$

f_Q function has been proposed to express the influence of the intracellular sulphur concentration on the photosynthetic growth

as follows:

$$f_Q = \frac{e^{(k(Q/Q_m))} - 1}{e^{(k)} - 1}(1 - f_{min}) + f_{min} \quad (8)$$

where $f_Q = 1$ if $Q > Q_m$. Q_m represents the maximal quota above which photosynthetic activity is not affected by the internal sulphur quota. f_{min} is the minimal value of f_Q when Q is null (the residual photosynthetic activity), and k is a parameter adjusting the exponential shape.

μ_s is the specific respiration rate (supposed to be constant). Y_{sx} is the yield of substrate conversion (g S/g of biomass) and k_s is the half saturation constant (g/L), describing the sulphur limitation of growth.

From Equations (2)–(4), it results in:

$$f(x) = \begin{bmatrix} f1 \\ f2 \\ f3 \end{bmatrix} = \begin{bmatrix} (f_Q) < \mu_G > X - \mu_s X \\ -Y_{sx}\left(< \mu_G > \frac{S}{S + k_s} \right) X \\ Y_{sx} < \mu_G > \frac{S}{S + k_s} - (f_Q) < \mu_G > Q \end{bmatrix}. \quad (9)$$

Simulated evolutions of X, S, and Q, using model parameters as reported in Fouchard et al.[1] are illustrated in Figures 1 and 2 in two different operating conditions: photosynthetic growth conditions (without sulphur deprivation) and H_2 production conditions (sulphur deprivation conditions). Initial conditions used in these simulations are reported in Table 1.

As can be seen in Figure 1, in the presence of a high amount of sulphur inside the culture medium, only the first phase (photosynthetic phase) was observed. The stationary phase appears after 6 days of cultivation as a result of light limitation. The internal quota has no influence on growth ($f_Q = 1$).

In the second simulated scenario, conditions inducing H_2 production were applied. As illustrated in Figure 2, the initial amount of sulphur concentration was ~8 time slower. The extracellular sulphur concentration was totally consumed after 2 days of cultivation, which represents the duration of the photosynthetic growth phase. Limitation induced by intracellular sulphur concentration occurred, as illustrated by the evolution of f_Q.

Sensitivity Functions

The objective of this study was to determine the parameters having the greatest influence on model outputs and to suggest a classification of them. This study allowed for the determination of the most important parameters and was used prior to the model parameter identification.

The sensitivity functions represent the influence of variations of each parameter on the output variables and are defined by the partial derivative of the output variable with respect to the parameter. The sensitivity functions provide information on the influence of parameters and the quality of identification.[5] Examples of calculation of the sensitivity functions can be found in the literature.[7,13] After sensitivity analysis, a model reduction could be conducted by removing the least significant parameters or fixing their values from the literature.

x_i $(i = 1, \ldots n)$ represents the state variables of the model and θ_j $(j = 1, \ldots p)$ represents the model parameters where p is the number of model parameters. The sensitivity functions reflect the sensitivity of the states x with respect to the parameter p, as defined by $\delta x_i/\delta\theta_j$. These functions are obtained by integrating the equations d/dt $(\delta x_i/\delta\theta_j)$ using the following equation:

$$\frac{d}{dt}\left(\frac{\partial x_i}{\partial \theta_j}\right) = \frac{\partial}{\partial \theta_j}\left(\frac{dx_i}{dt}\right). \quad (10)$$

The dynamics of states are given by:

$$\frac{dx_i}{dt} = \tau_i(x, u, \theta) \quad (11)$$

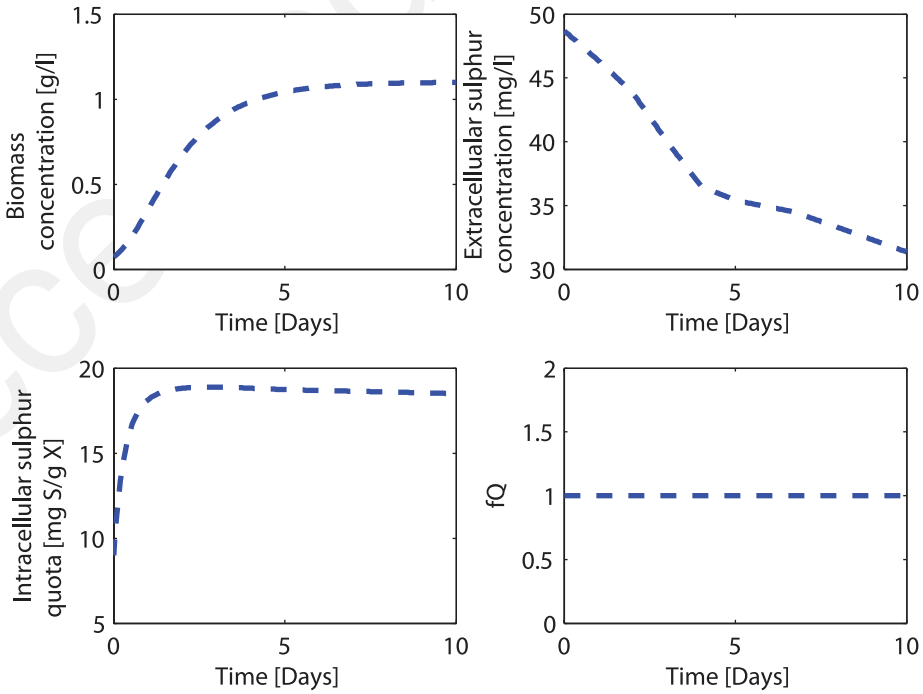

Figure 1. Evolution of state variables of the model (X, S, Q) and f_Q—growth phase.

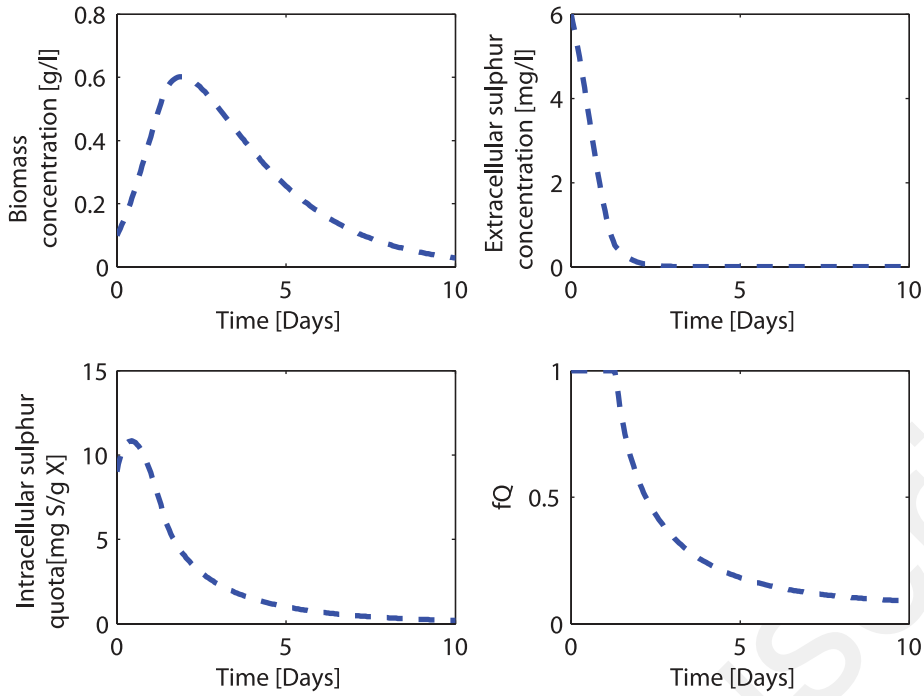

Figure 2. Evolution of state variables of the model (X, S, Q) and f_Q—sulphur deprivation phase.

where τ_i represents the n differential equations of state variables, and x_i and τ_i are non-linear functions. Thus, from Equations (10) and (11), we obtain:

$$\frac{\mathrm{d}}{\mathrm{d}t}\left(\frac{\partial x_i}{\partial \theta_j}\right) = \frac{\partial \tau_i}{\partial \theta_j} + \sum_{k=1}^{n} \frac{\partial \tau_i}{\partial x_k}\frac{\partial x_k}{\partial \theta_j}. \tag{12}$$

The calculation of sensitivity functions was done by solving a system of ordinary differential equations of dimension $n\ (p+1)$. However, the model parameters are likely to have quite different orders of magnitude, leading to numerical difficulties in the analysis of model sensitivity compared to the parameters. To overcome this problem, normalized sensitivity functions were used.[14]

Normalized sensitivity functions can be classified according to their parameters influence and determine the most influential parameters.

The expressions of the sensitivity functions of the model were deduced from Equations (10) and (12) as follows:

$$\frac{\mathrm{d}}{\mathrm{d}t}\left(\frac{\partial x_i}{\partial \theta_j}\right) = \frac{\partial \tau_i}{\partial \theta_j} + \frac{\partial \tau_i}{\partial X}\frac{\partial X}{\partial \theta_j} + \frac{\partial \tau_i}{\partial S}\frac{\partial S}{\partial \theta_j} + \frac{\partial \tau_i}{\partial Q}\frac{\partial Q}{\partial \theta_j}. \tag{13}$$

The index i of the state variables denotes the three states (X, S, Q) and j denotes the model parameter.

Table 1. Conditions of simulations of the sensitivity functions

Non-limited growth case	Sulphur deprivation case
$[X_0;\ S_0;\ I_0] =$ [0.072 g/L; 48.7 mg/L; 110 μmole m^{-2} s^{-2}]	$[X_0;\ S_0;\ I_0] =$ [0.099 g/L; 6 mg/L; 110 μmole m^{-2} s^{-2}]

Simulation time: 10 days.

Cost Function Minimization

Classical least-squares estimator (LS) is a popular approach that is based on the assumption that the measurement errors have constant (but possibly unknown) standard deviation.13′

$$J_{\mathrm{LS}}(\theta) = \sum_{t=1}^{N} \left(y_{\mathrm{exp}}(t) - y_{\mathrm{sim}}(t,\theta)\right)^2 \tag{13′}$$

where J_{LS} is the objective function, y_{exp} are the collected measurements, y_{sim} are the model-predicted outputs, θ represents the parameters to be determined and N is the number of measurements.

For weighted least-squares (WLS), if the variance of the measurement errors is time varying, then the previous expression generalizes to:

$$J_{\mathrm{LS}}(\theta) = \sum_{t=1}^{N} \left(\frac{y_{\mathrm{exp}}(t) - y_{\mathrm{sim}}(t,\theta)}{\sigma_t}\right)^2. \tag{14}$$

Extended Kalman Filter

The Kalman filter is the most widely adopted state estimation technology for non-linear systems. We chose this approach for our problem, but many other approaches could also be used. The dynamics of a non-linear bioprocess can be expressed in the following general form:

$$\dot{x}(t) = f[x(t)] + w(t), \quad x(t)|_{t=0} = x_0 \tag{15}$$

$$Y(t) = h[x(t)] + v(t) \tag{16}$$

where $x(t)$ is the state vector with an initial value of x_0, $Y(t)$ is the measurement vector, $w(t)$ is the system noise (representing modelling error and unknown disturbances), and $v(t)$ is the measurement noise. Both system and measurement noises are assumed to be independent, random white noises with zero mean with corresponding covariance matrices Q and R. When the

measurements are taken continuously in time, the extended Kalman filter (EKF) algorithm for calculating the optimal state estimate $\hat{x}$ based on the available measurement up to current time t is given by[15]:

$$\dot{\hat{x}}(t) = f[\hat{x}(t)] + K(t)\{Y(t) - h[\hat{x}(t)]\}, \quad \hat{x}(t)|_{t=0} = \hat{x}_0 \tag{17}$$

where $K(t) = P(t)C(t)R^{-1}$, $K(t)$ is the filtering gain matrix, and $P(t)$ is the covariance matrix of filtering error, satisfying the following matrix Riccati equation:

$$\dot{P}(t) = A(t)P(t) + P(t)A^T(t) - K(t)RK^T(t) + Q, \quad P(t)|_{t=0} = P_0 \tag{18}$$

where: $A(t) = \frac{\partial f[x(t)]}{\partial x^T(t)}|\hat{x}(t)$, $C(t) = \frac{\partial h[x(t)]}{\partial x^T(t)}|\hat{x}(t)$.

RESULTS AND DISCUSSIONS

Results of Sensitivity Analysis

Our study focused on the influence of parameters on the three state variables of the model, biomass, sulphur, and sulphur internal quota, supposing their three measures could be considered for the parametric identification.

As described before, we distinguish the case of growth in non-limiting conditions with respect to sulphur, but in limiting light conditions, from the case of growth under sulphur deprivation conditions, where the rate of growth depends on both the incident light flux and the intracellular quota. From the mathematical viewpoint, the difference lies in the term f_Q (Equation (8)), which in the first case is equal to 1.

The vector of parameters θ was:

- $\theta_j = [\mu_{max}, K_I, \mu_s, k_s, Y_{sx}]$—in the case of growth without sulphur limitation, that is called hereafter the non-limited growth case.
- $\theta_j = [\mu_{max}, K_I, \mu_s, k_s, Y_{sx}, f_{min}, k, Q_m]$—in the case of growth in conditions leading to sulphur deprivation, that is called hereafter the sulphur deprivation case, it adds the parameters involved in the function (f_Q).

Given the complexity of the analytical calculation of the equations, the sensitivity functions were determined through the symbolic software Mathematica®, and then the integration was done numerically in Matlab®.

The analysis of the sensitivity functions was applied in both cases mentioned above. The initial conditions used in simulation for each case were chosen based on normal conditions placing the system into the desired operating scenario. These conditions are reported in Table 1.

The sensitivity functions in the non-limited growth case and the sulphur deprivation case are shown in Figures 3 and 4, respectively. We note that normalized sensitivity functions allowed comparing the relative influence of parameters with respect to a state variable and not between different state variables because of their different units. Consequently, for a given state variable, the parameter that has the most sensitivity is one that has the highest absolute value in the same case. We note that we cannot compare the sensitivity of the parameters of a state variable in two different cases.

In the non-limited growth case (Figure 3), we note the strong influence of μ_{max}, K_I, and μ_s in the same proportions on X, S, and Q, indicating that these three parameters have to be identified simultaneously from all available experimental data. In turn, there is no influence of Y_{sx} and k_s parameters on X and poor influence on S. This allowed decoupling the identification of these last two parameters of the rest. We note that the most sensitive parameters were the kinetic parameters of the photosynthetic growth rate μ_G.

In the sulphur deprivation case, the sensitivity functions (Figure 4) presented a maximum that corresponds to the moment when the internal sulphur quota reached its maximum.

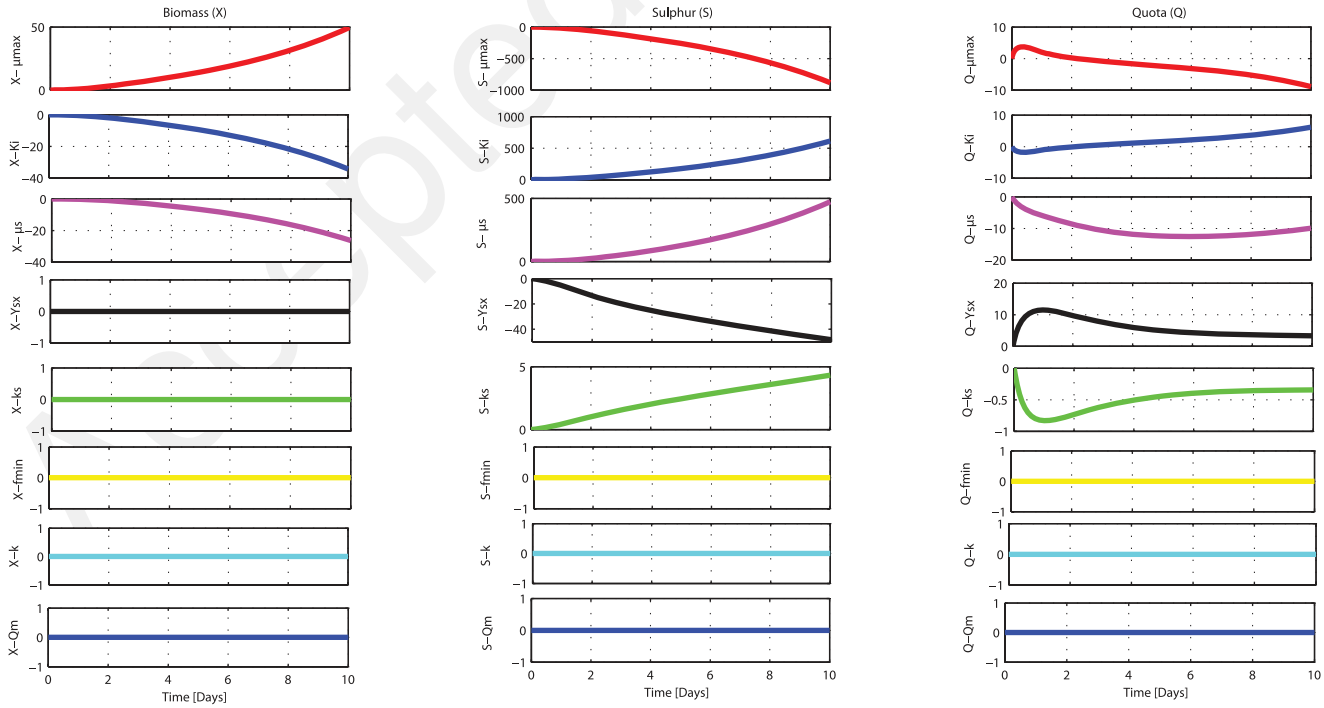

Figure 3. Evolution of sensitivity functions—non-limited growth case.

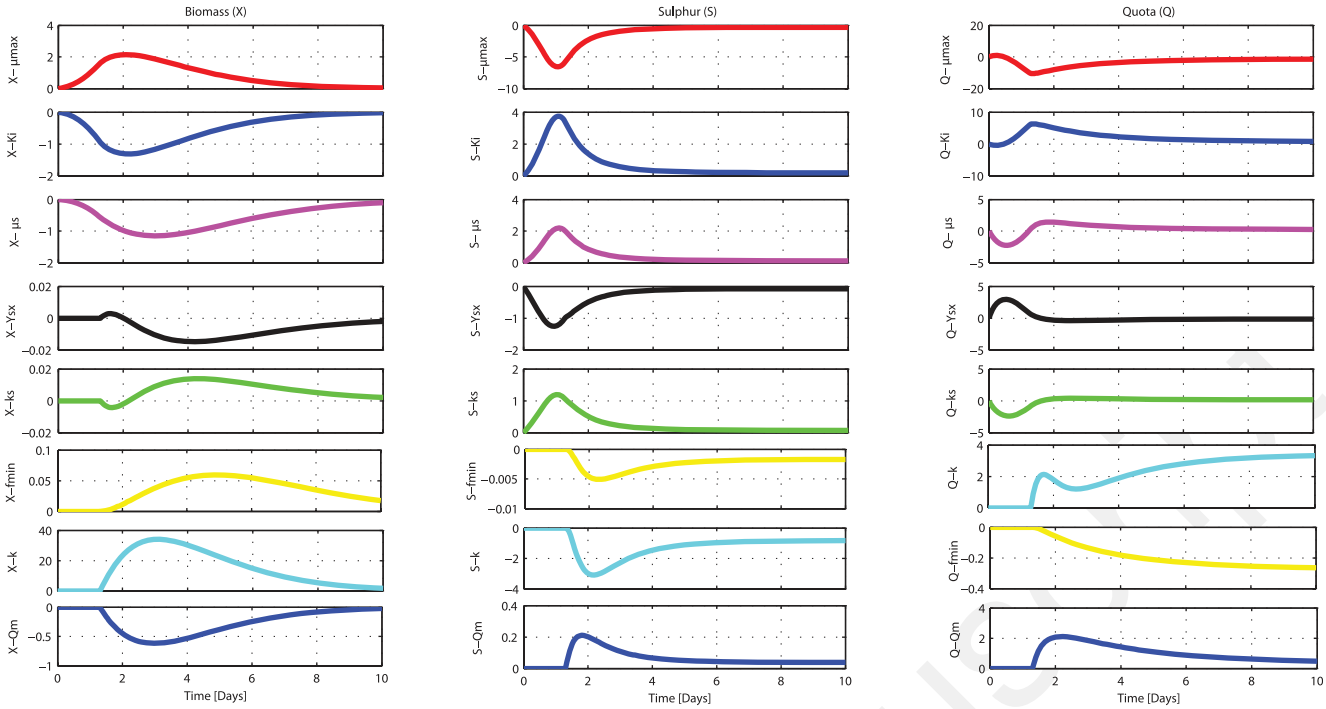

Figure 4. Evolution of sensitivity functions—sulphur deprivation case.

Furthermore, the parameters μ_{max}, K_I, and μ_s were also influential in sulphur deprivation phase, peaking when the internal quota was consumed due to the lack of extracellular sulphur.

While in the non-limited growth case the sensitivity functions increased with time, in the sulphur deprivation case we noted the presence of peaks in precise moments. These peaks indicate that an important number of measurements have to be performed during this period for accurate parameter identification.

Regarding the specific parameters of the sulphur deprivation case, the parameter f_{min} showed very little influence compared the other two parameters (k and Q_m). The k parameter has a maximum influence after 2 days of cultivation on X and S. Q_m influenced more on Q than on X and S. As expected, the measurement of the intracellular sulphur quota would improve the identifiability of this parameter.

For the non-limited growth case, the absolute value of the sensitivity functions are exponentially increasing, and all parameters have the same shape of curve except on Q. On the other hand, for the sulphur deprivation case the value of the sensitivity functions are peak sensitivity values and all parameters have the same shape of curve. To summarize, a classification of parameters according to their influence is proposed in Table 2. A score comprised between 1 and 8 was awarded, and the parameter that has the higher influence is that which has the higher score.

Based on this analysis, an identification methodology, in few steps, could be proposed as follows:

- μ_{max}, K_I, μ_s have to be identified first on X and S experimental data obtained during a non-limited growth case
- In a second step, k_s and Y_{sx} have to be identified on S data, in sulphur limitation conditions after 5 days of cultivation. This choice is justified because these two parameters (k_s and Y_{sx}) have sensitivity pretty close to the three most influential parameters (μ_{max}, K_I and μ_s). Therefore, an improvement may be possible by optimizing the k_s and Y_{sx} parameters in the case of sulphur limitation conditions.
- Then, Q_m and k parameters have to be identified in sulphur deprivation conditions using experimental data of X, between 2 and 7 days of cultivation (corresponding to the decay phase of biomass. Q measurements should significantly increase the accuracy of this parameters identification.

Since the intracellular sulphur quota Q remains nearly constant in the non-limited growth case, its measurement does not provide any additional information with respect to X and S, as was expected.

Sensitivities functions in sulphur deprivation case were significantly lower for the parameters μ_{max}, K_I, μ_s, Y_{sx}, and k_s (Figures 3 and 4), which confirms the choice to identify the parameters in a few steps.

Dependencies Between Parameters

To perform reliable parameter identification, it is important to check if there are dependencies between parameters. This study

Table 2. Classification of the influence of parameters in both phases

	Non-limited growth case			Deprivation case		
Parameter	Biomass	Sulphur	Quota	Biomass	Sulphur	Quota
μ_{max}	8	8	8	6	6	6
μ_s	6	6	6	4	2	3
K_I	7	7	7	5	5	5
Y_{sx}	0	5	5	3	4	4
k_s	0	4	4	2	3	2
k	0	0	0	8	8	8
Q_m	0	0	0	7	7	7
f_{min}	0	0	0	1	1	1

allows for determining parameters, which are not individually identifiable, and where applicable, the two parameters can be replaced, for example, by their ratio (if the model equations allow us to distinguish this report from the rest of the parameters).

The calculation of the determinant of the Gram matrix gives valuable information on the dependencies between the parameters: if the determinant is null, the parameters are linearly dependent; if not, the parameters are linearly independent and therefore identifiable. Luenberger[16] defines the Gram matrix of normalized sensitivity functions (Equation (19)) where S_θ is the sensitivity function of each parameter (θ):

$$G = \begin{bmatrix} \frac{1}{T}\int_0^T S_{\theta_1}^2 \mathrm{d}t & \frac{1}{T}\int_0^T S_{\theta_1}S_{\theta_2}\mathrm{d}t & \cdots & \frac{1}{T}\int_0^T S_{\theta_1}S_{\theta_{p-1}}\mathrm{d}t\,\frac{1}{T}\int_0^T S_{\theta_1}S_{\theta_p}\mathrm{d}t \\ \frac{1}{T}\int_0^T S_{\theta_2}S_{\theta_1}\mathrm{d}t & \frac{1}{T}\int_0^T S_{\theta_2}^2\mathrm{d}t & \frac{1}{T}\int_0^T S_{\theta_2}S_{\theta_3}\mathrm{d}t & \cdots \\ \vdots & \vdots & \ddots & \\ \frac{1}{T}\int_0^T S_{\theta_{p-1}}S_{\theta_1}\mathrm{d}t & \vdots & & \frac{1}{T}\int_0^T S_{\theta_{p-1}}^2\mathrm{d}t \\ \frac{1}{T}\int_0^T S_{\theta_p}S_{\theta_1}\mathrm{d}t & \frac{1}{T}\int_0^T S_{\theta_p}S_{\theta_2}\mathrm{d}t & \cdots & \frac{1}{T}\int_0^T S_{\theta_p}S_{\theta_{p-1}}\mathrm{d}t\,\frac{1}{T}\int_0^T S_{\theta_p}^2\mathrm{d}t \end{bmatrix} \quad (19)$$

The calculation of the determinant of the Gram matrix corresponding to the two vectors of selected parameters with respect to state variables X, S gave a nonzero response. It could be concluded that the parameters μ_{max}, K_I, and μ_s are linearly independent with respect to the biomass X and sulphur S concentrations.

During sulphur deprivation phase, the calculation of the Gram matrix for the vector of parameters selected for re-identification (k, Q_m) gives a non-zero response of the two variables X and S. So we can conclude that these parameters are identifiable.

Conditioning of the Gram Matrix

Calculation of determinant of the Gram matrix shows only if the parameter is identifiable or not, while calculating the conditioning of the Gram matrix gives the degree of identifiability of parameters. So, from the calculation of the conditioning Gram matrix, the best operating conditions for identifying the selected parameters could be found.

A study was conducted to find the best operating condition with respect to the incident light (I_0) ranging between 50 and 800 μmol/m^2/s.

From Figure 5, it follows that the best results (lower conditioning of the Gram matrix) with respect to S were found for incident light (I_0) ranging between 200 and 600 μmol/m^2/s. Best identification conditions using X alone is found for the lowest incident light intensity $I_0 = 50$ μmol/m^2/s, and for S the optimal value is to $I = 300$ μmol/m^2/s.

In the sulphur deprivation case, analysis of the two parameters chosen for the identification (k, Q_m) showed that we have better identification conditions for an incident light intensity $I_0 = 190$ μmol/m^2/s using two measured states, X and S (Figure 6). In the case of X alone, the best operating condition of the incident light was $I = 50$ μmol/m^2/s, and for S its value is $I = 250$ μmol/m^2/s.

Note that the results obtained in both phases are similar. The optimal incident light conditions for the identification of X is the lowest value for $I = 50$ μmol/m^2/s, and for S it is between 250 and 300 μmol/m^2/s.

Results of Cost Function Minimization

Simulation of the model variables—experimental data

We will compare the simulation of the model variables to experimental data.[17,18] The experimental conditions are presented as follows in Table 3.

The first two experiments (Growth experiments 1 and 2) allow us to analyze the growth phase on a medium autotrophic CO_2—only carbon source under conditions of non-limited sulphur. The other two experiments were performed on an autotrophic medium limited in sulphur. These experiments were conducted at different light intensity with the aim of characterizing the growth of these microalgae at the growth kinetics and gas production.

The model presented above was used to describe the evolution of a culture of microalgae in batch mode. The results of the comparative evolutions between the model and experimental data under the conditions of Growth experiments 1 and 2 are presented in Figures 7 and 8. The simulation shows that the model predicts that the sulphur is totally consumed. This prediction leads to a reduction of internal quota, and thus the passage in phases 2 and 3, which are not observed experimentally. Note also that the growth kinetics (X) are overestimated in both cases.

Deprivation experiments 3 and 4 were conducted under operating conditions leading to the production of H_2 and as a result the consecutive passes by three phases. The simulation of the model state variables X and S compared with experimental data are shown in Figures 9 and 10. We notice an overestimation of growth rate, as before. In both cases, the model predicts that the sulphur is totally consumed. This prediction affects the rest of the variables,

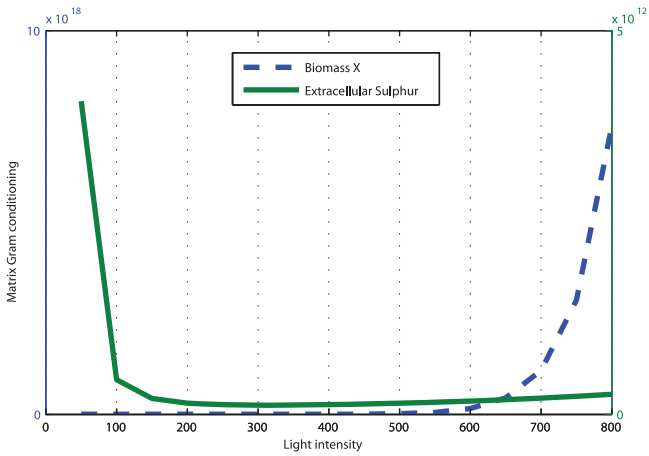

Figure 5. Light optimal condition for the identification in photosynthetic growth phase.

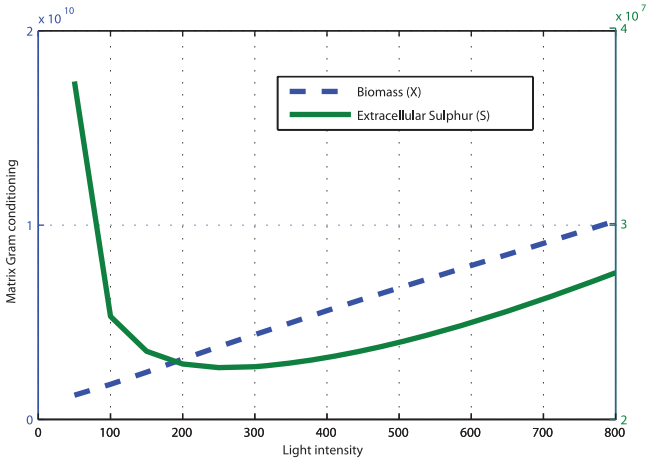

Figure 6. Light optimal condition for the identification—sulphur deprivation phase.

including causing a decrease in intracellular sulphur quota internally. Given this gap between the model and experimental data, we must conduct an identification of parameters.

Parameter identification, non-limited growth case

The second step consists of identifying the dominant parameters that were calculated in the first step with available measurements. The choice of these parameters is due to their significant influence in their mode of operation illustrated by the values of the normalized sensitivity functions. This identification is the result of minimizing the sum of squared deviations between experimental data and the simulated corresponding values. The optimization of this criterion is performed with an algorithm from Matlab® using the *fmincon* function.

The chosen parameters in a non-limited growth case are μ_{max}, K_I, and μ_s. The parameter identification was performed using

Table 3. Operating conditions and initial experiences

Experiment	Initial Biomass (g/L)	Initial sulphur (mg/L)	Initial intensity (μmole/m^2/s)
Growth experiment 1	0.072	48.70	110
Growth experiment 2	0.181	133.9	300
Deprivation experiment 3	0.099	6	110
Deprivation experiment 4	0.1315	22.28	500

experimental data from Growth experiment 1, whose operating conditions are presented in Table 3. The identification procedure was conducted by giving more importance to the X variable than the variable S, by weighting in this regard the optimization criterion.

The parameter values obtained after the identification are $\mu_{max} = 0.0685\,h^{-1}$, $\mu_s = 0.0074\,h^{-1}$ and $K_I = 81.4019\,\mu mol/m^2/s$. The simulation results of the new values obtained by the identification are shown in Figure 11.

Figure 11 shows a very good fit to describe the evolution of biomass concentration in the growth phase. In the extracellular concentration of sulphur, we see an improvement during the first 5 days, and a degradation due to the model prediction of totally consumed sulphur in the medium.

To improve the prediction of S, we have identified parameter Y_{sx} using only the evolution of S. A smaller value was found for Y_{sx} (8.631) compared to its initial value in the non-limited growth phase ($Y_{sx} = 20.6$). This value has improved the prediction of S at the end of the culture because S is not totally consumed (Figure 12).

We can conclude that the identification of parameters in the non-limited growth case gave a perfect fit for X. However, although it could solve the problem corresponding to the prediction of the total consumption of S in the medium, we lose the good fit that we had in the first six days of the extracellular sulphur concentration. This validates the low influence of the parameter Y_{sx} compared to other parameters identified.

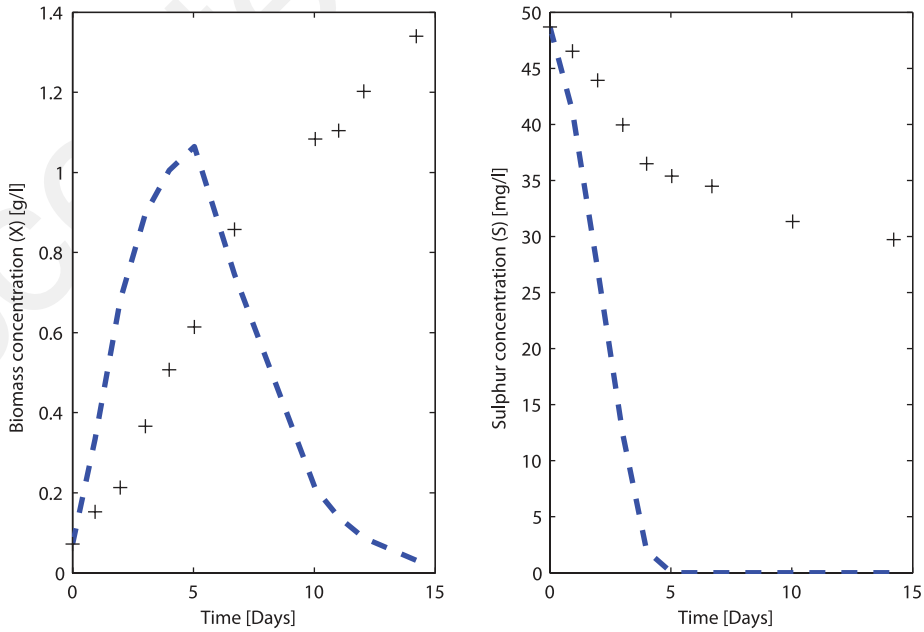

Figure 7. Evolution of the model variables (X, S) ---, and experiment (+)—Growth experiment 1.

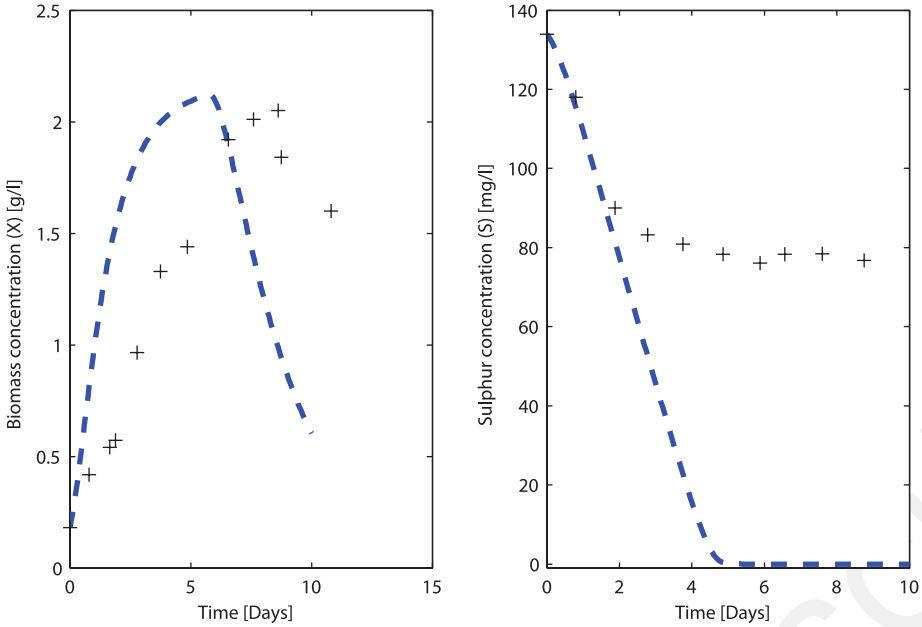

Figure 8. Evolution of the model variables (*X*, *S*) ---, and experiment (+)—Growth experiment 2.

Validation of parameters identified in the non-limited growth case

To validate the model with new parameter values identified, we simulated the model in other operating conditions corresponding to the experimental data of Growth experiment 2, as presented in Table 3. Similar to the biomass concentration, Figure 13 shows a good fit between the model and experimental data, except for the last two points which are due to a decrease in light intensity that was not taken into consideration in the model. However, we found an overestimate of the evolution of the extracellular sulphur concentration.

The model with the new parameters identified in the growth phase was used to simulate the operating conditions corresponding to experimental data from Deprivation experiments 3 and 4 to see the impact of these parameters in the deprivation phase.

Figures 14 and 15 show a good improvement in the prediction of the model (compared to experimental data of the original model) for the biomass concentration and extracellular sulphur. However, the deprivation phase, characterized by a decrease in biomass, was not adequately predicted. In view of these results, we conducted an identification of specific parameters of the deprivation phase, k and Q_m.

Parameter identification—sulphur deprivation case

The parameter identification was performed using experimental data from Deprivation experiment 4, whose operating conditions are presented in Table 3. The function f_Q takes into account, by the exponential form, the photosynthetic activity by the intracellular sulphur quota. We noted that the photosynthetic activity occurs for

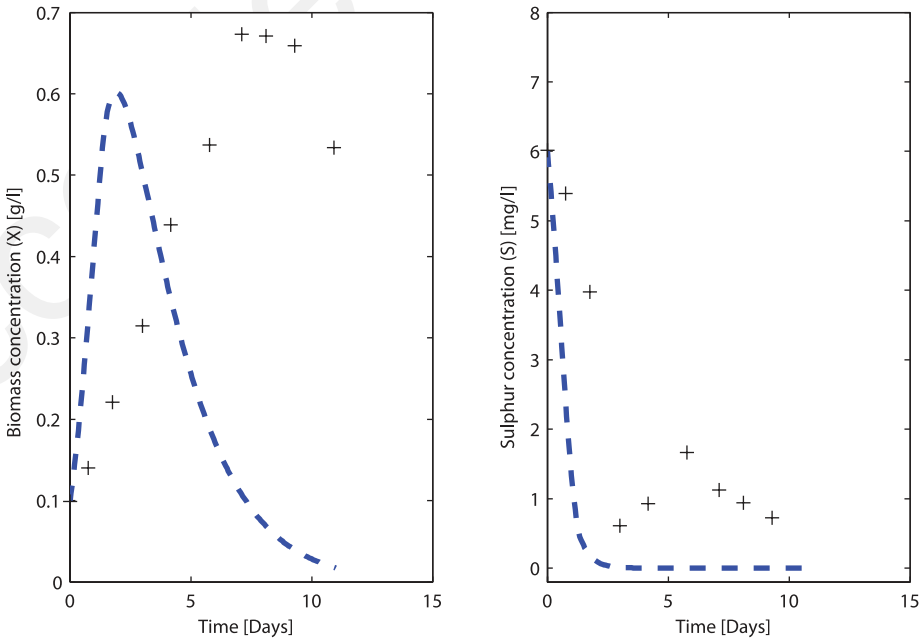

Figure 9. Evolution of the model variables (*X*, *S*) ---, and experiment (+)—Deprivation experiment 3.

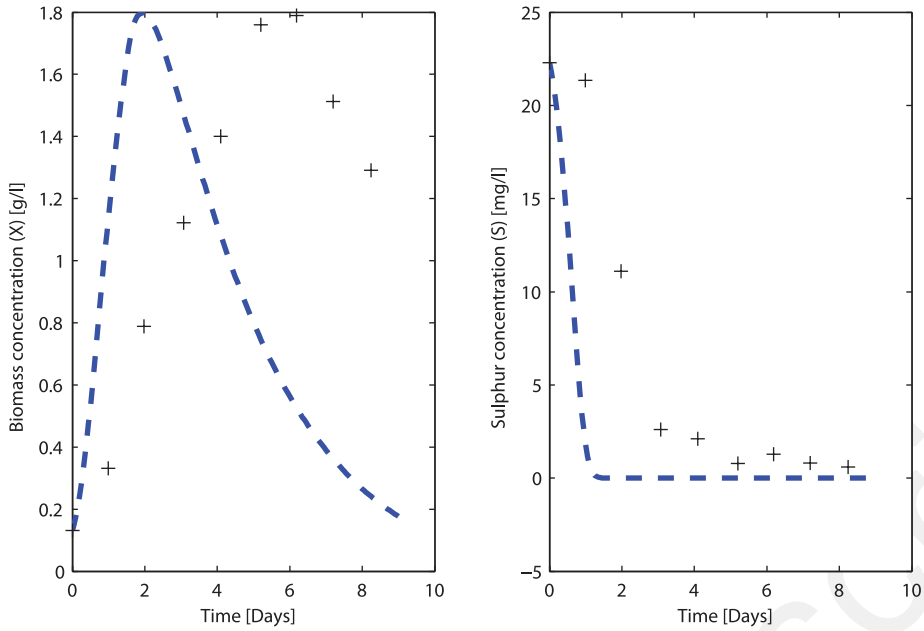

Figure 10. Evolution of the model variables (*X*, *S*) ---, and experiment (+)—Deprivation experiment 4.

at least 24 h in the experimental conditions cited above.[1] It was observed that when the value of the parameter k exceeds 10, the photosynthetic activity is not in accordance with experimental data. To solve this problem, the value of k was limited to 10 in the algorithm optimization. The parameter values obtained after identification are $k = 7.9575$ and $Q_m = 8.3145$ mg S/mg X. The simulation results using the new values obtained after identification are shown in Figure 16. We can see that the identification of parameters k and Q_m correctly predicts the deprivation phase and considers the decrease in biomass concentration. Similar to the concentration of sulphur, we found a good fit between the model and experimental data.

The new parameter values identified in the S deprivation case using the operating conditions of Deprivation experiment 4 were tested on Deprivation experiment 3 to validate them. The evolution of biomass concentration shows a gap between the kinetic model and experimental data (Figure 17). The decrease in biomass concentration starts before the experimental data. In fact, the simulation shows that the biomass concentration starts to decrease after reaching a value of 0.51 g/L. Otherwise, the experimental data shows that the decrease in biomass concentration begins after reaching the value 0.69 g/L. The sulphur concentration maintained a good fit.

After an analysis of the result of the parameters identified, we noted that the new value of μ_{max} is less than the value identified on

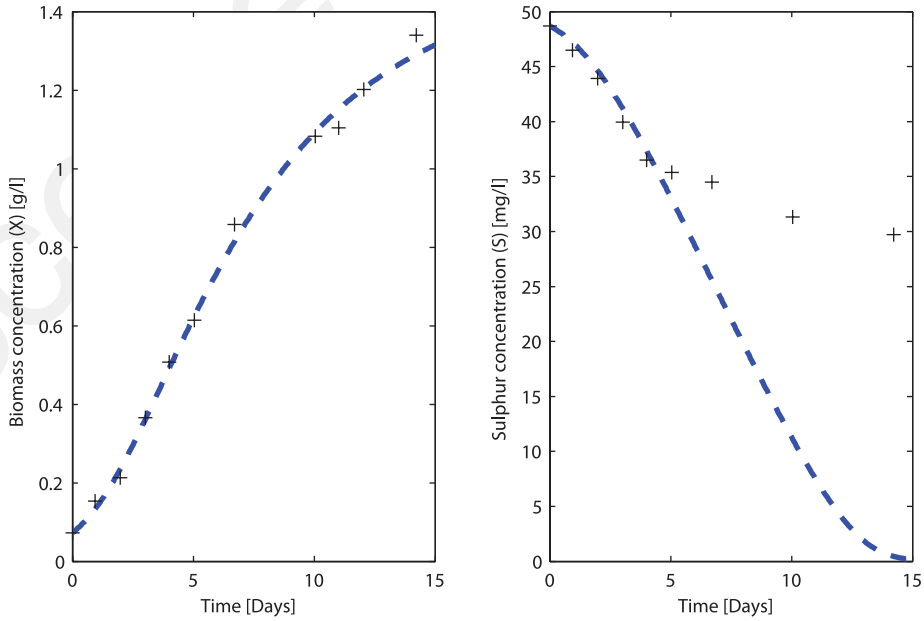

Figure 11. Comparison between the simulation state variables of the model and the experimental data using the re-identified values, μ_{max}, μ_s and K_I—Growth experiment 1.

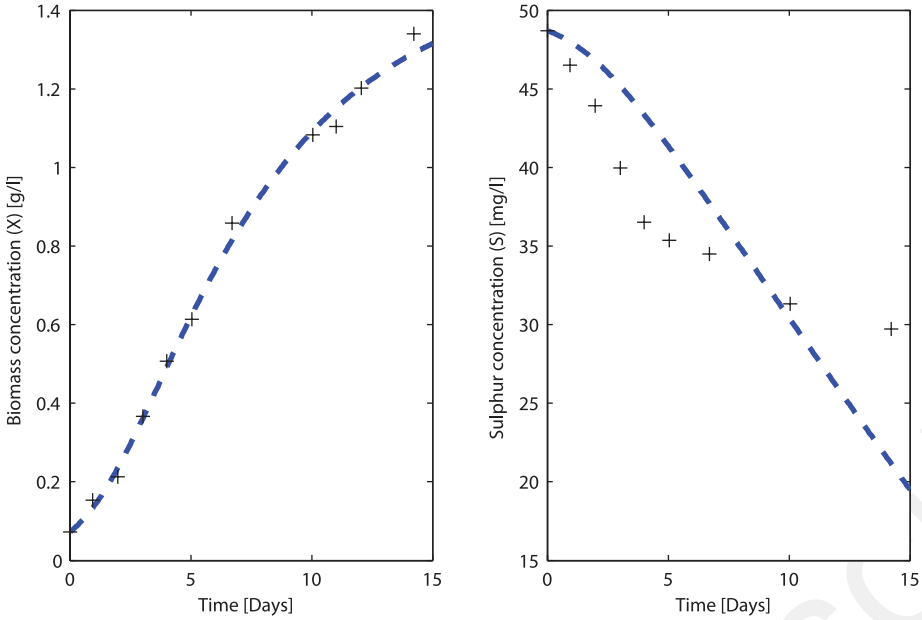

Figure 12. Comparison between the simulation state variables of the model and the experimental data using the re-identified values, μ_{max}, μ_s, K_I, and Y_{sx}—Growth experiment 1.

dedicated experiments in chemostat.[4] Using the model with the new values results in the specific rate of growth that are not verified by chemostat, as shown in Figure 18, and therefore that does not meet the biological significance of this parameter.

To understand this result, we looked at the impact that could have the optical parameter E_a in Equation (6), considered until now as perfectly known and constant. However, recent work[19] shows that the parameters E_a change significantly depending on the values of the light intensity, as shown in Table 4. These values were obtained under conditions of physical limitation by light ($\gamma = 1$) in the PBR, cultivating the microalgae *C. reinhardtii*.

Thus, we conducted a simulation study to determine the impact of these parameters on the attenuation profile of the light intensity at depth of culture. As shown in Figures 18 and 19, the parameter E_a has a very important impact on the growth rate.

We see that the attenuation of the light intensity profile G_z decreases with increasing E_a. Thus, the values of growth rates calculated with these profiles will be reduced accordingly. The

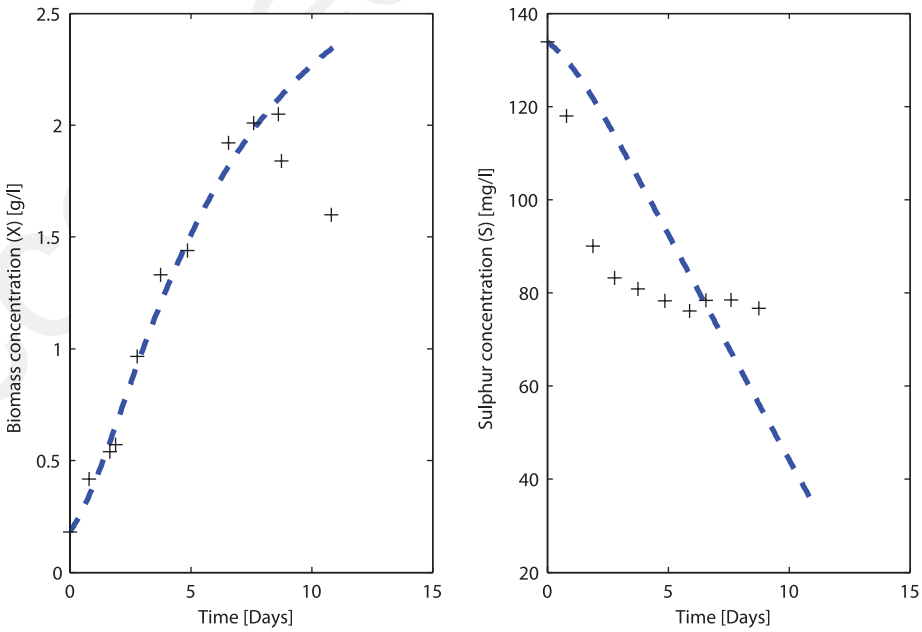

Figure 13. Comparison between the simulation state variables of the model and the experimental data using the re-identified values, μ_{max}, μ_s, K_I—Growth experiment 2.

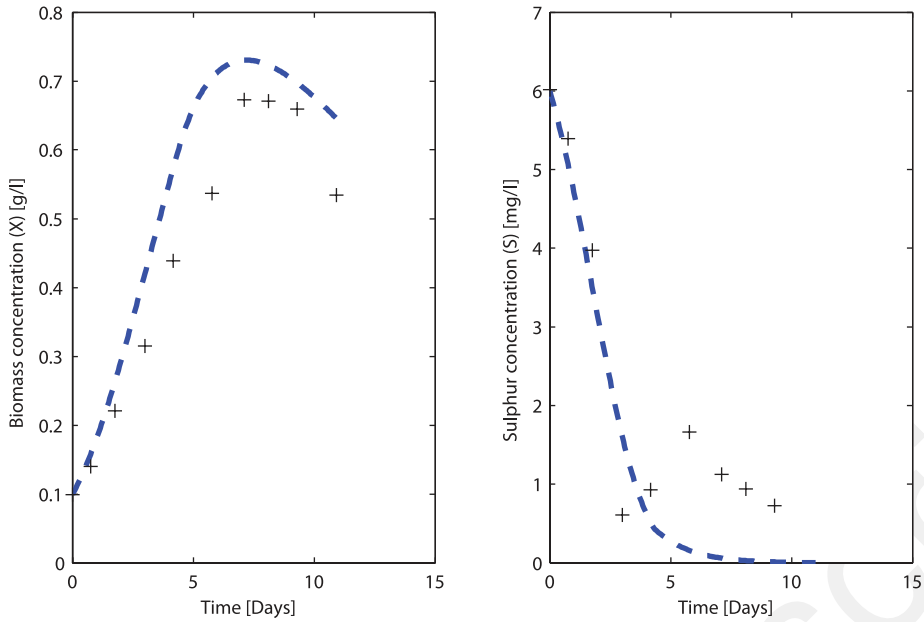

Figure 14. Comparison between the simulation state variables of the model and the experimental data using the re-identified values, μ_{max}, μ_s, K_I— Deprivation experiment 3.

value of E_a used in the identification step was $E_a = 220\,m^2kg^{-1}$,[4] while the "true" average value measured by Takache is $172\,m^2kg^{-1}$.[19] As a result, the low value of μ_{max} obtained by parametric identification compensates for uncertainties on the optical parameters including the parameter E_a.

The value of the parameter identified as K_I is very close to the old value. For the parameters k and Q_m that appear in the equation f_Q (Equation (8)), we found $k = 3.8996$ is larger compared to the old value (0.3389) calculated by regression on experimental data related to f_Q, and $Q_m = 6.7449$, which is a little smaller than the former value of 7. With this new value of k, the effect of limiting intracellular quota (Q) is larger.

Results of Extended Kalman Filter Applied to PBR

Observability of the system

The verification of the observability property throughout the state space is necessary before the construction of the observer. Recall that a nonlinear system is uniformly observable if the following observability matrix is full rank:

$$\frac{\partial}{\partial x}[h\,L_f h\,L_f^2 h \cdots L_f^{n-1} h]^t \tag{20}$$

where $h(x)$ as the system output, and $L_f h(x)$ as the Lie derivative of the function $h(x)$ along a vector field $f(x)$. The system output is

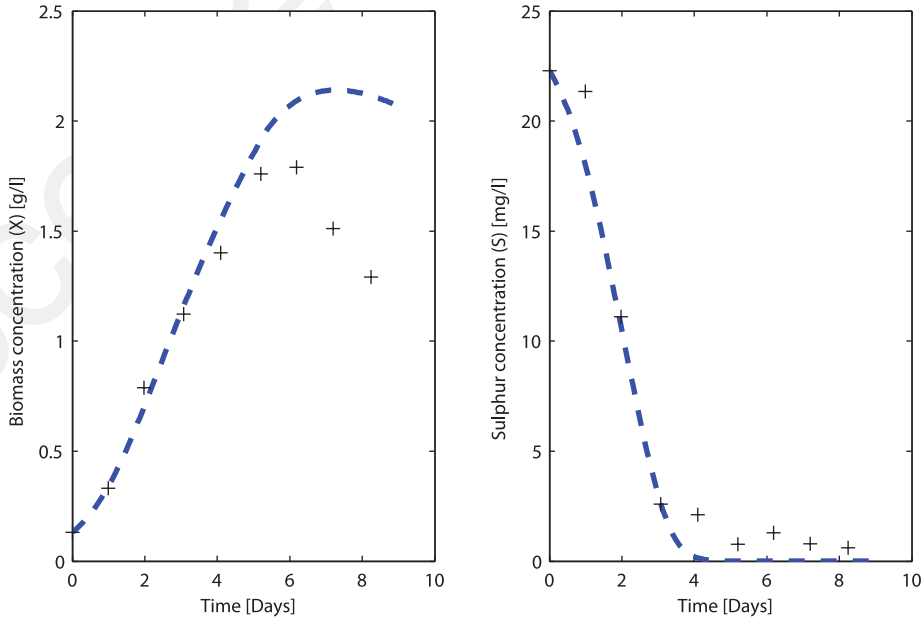

Figure 15. Comparison between the simulation state variables of the model and the experimental data using the re-identified values, μ_{max}, μ_s, K_I— Deprivation experiment 4.

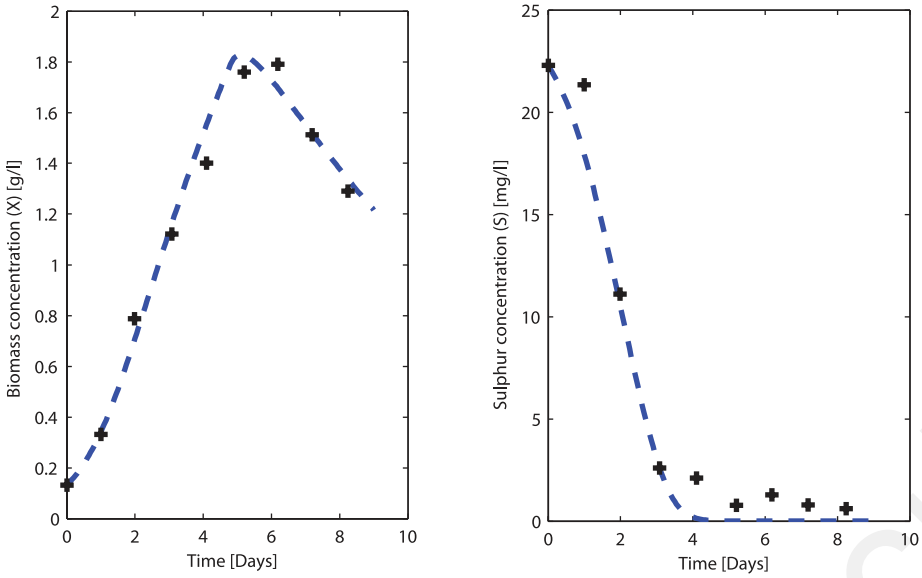

Figure 16. Comparison between the simulation state variables of the model and the experimental data using the re-identified values, Q_m, k—Deprivation experiment 4.

equal to the measurement of biomass concentration:

$$h(x) = X. \tag{21}$$

Thus, following observability matrix is obtained:

$$\begin{bmatrix} 1 & 0 & 0 \\ \dfrac{\partial f_1}{\partial X} & 0 & \dfrac{\partial f_1}{\partial Q} \\ \dfrac{\partial}{\partial X}\left(\dfrac{\partial f_1}{\partial X} f_1 + \dfrac{\partial f_1}{\partial Q} f_3\right) & \dfrac{\partial}{\partial S}\left(\dfrac{\partial f_1}{\partial X} f_1 + \dfrac{\partial f_1}{\partial Q} f_3\right) & \dfrac{\partial}{\partial Q}\left(\dfrac{\partial f_1}{\partial X} f_1 + \dfrac{\partial f_1}{\partial Q} f_3\right) \end{bmatrix}. \tag{22}$$

The determinant of the observability matrix is function of the biomass concentration (X), incident light flux density (I_0) and the internal sulphur quota (Q).

Recall that the model used here corresponds to a modified Droop model describing sulphur deprivation effect on the microalgae growth. This is modelled by means of the function f_Q varying between 0 and 1, depending on Q, as illustrated in Figure 21. In the case of the non-limitation of intracellular sulphur quota (extracellular sulphur concentration is sufficient in the culture medium), the term $f_Q = 1$. In this case, $\delta f_1/\delta Q = 0$ and the determinant of the observability matrix becomes equal to zero.

When $f_Q < 1$, the determinant is defined for any value of Q, unless $X = 0$ and $I_0 = 0$. It does not vanish on the whole state space,

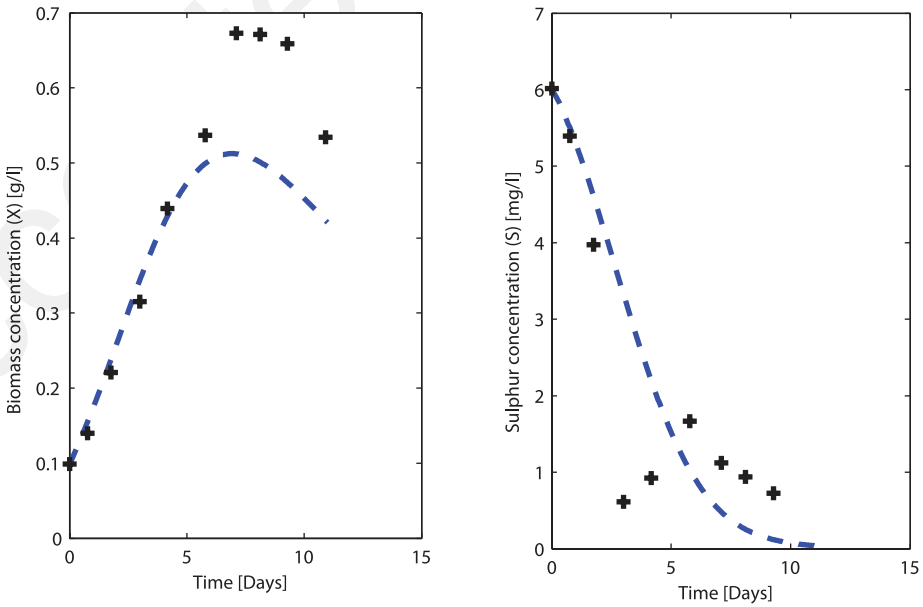

Figure 17. Comparison between the simulation state variables of the model and the experimental data using the re-identified values, Q_m, k—Deprivation experiment 3.

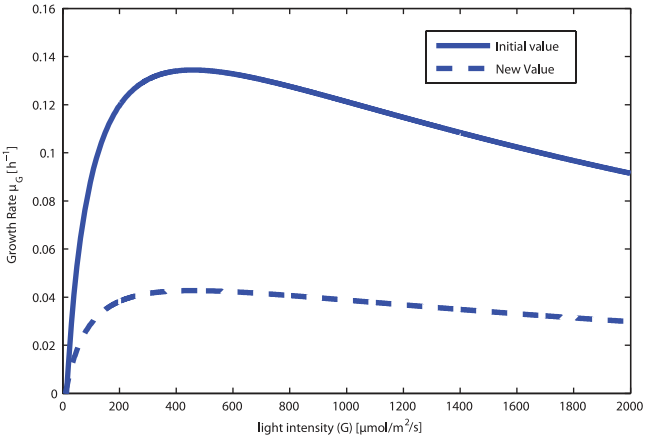

Figure 18. Growth rate as a function of the light intensity.

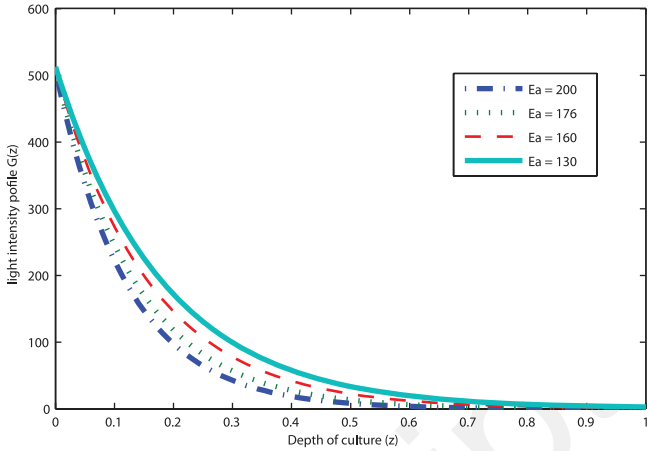

Figure 19. Light intensity profile of the luminous flux G_z for different values of E_a.

as illustrated in Figure 20, representing the set of values taken by the determinant in the practical range of biomass concentration and incident light flux density (I_0). This analysis allows us to conclude that the observability of the system is uniform in this case. However, it may be noted that for low values of biomass concentration and incident light flux intensities, the determinant is very close to zero and its minimum value is -5.78×10^{-7}.

Thus, we can conclude the non-observability of the system under non-limiting sulphur conditions. In limiting conditions (corresponding to hydrogen producing conditions) the system is observable. An illustration that gives the evolution of the observability matrix rank with time during a batch is presented in Figure 21. It can be noticed that during the first 5 days of cultivation, when extracellular sulphur concentration is not growth limiting, the rank of the observability is 1 and it becomes 3 when f_Q starts to decrease.

Experimental materials and methods

Experiments were carried-out in a laboratory photobioreactor equipped with data acquisition system developed in a LabVIEW® environment. The extended Kalman filter as well as the indirect measurement of the biomass concentration were developed using LabVIEW® environment. Experimental data—inlet and outlet gas flow rates and O_2, CO_2 gas compositions measured using a mass spectrometer (Pfeiffer Vacuum PrismaPlus® QMG 220)—are integrated into a *Matlabscript*.[1] In this node, gas mass balance equations are used to provide on-line indirect measurement of biomass concentration. A graphical representation of the system is given in Figure 22.

Biomass estimation

A major difficulty for process control is the reliability of the measurements. In the case of the Kalman filter, whose role will be to rebuild the quantities that cannot be measured on-line (internal quota and extracellular sulphur concentration), a reliable knowledge of the biomass concentration in real time is necessary. Several techniques are available to evaluate biomass, such as dry weight measurement measured offline (this method is considered as a reference method). Other methods exist that provide on-line measurement, such as physical sensors like the dielectric spectroscopy, optical sensors, infrared spectroscopy, and fluorescence physical sensors.

It is possible to use other variables measured in the bioreactor to estimate the biomass concentration, including the use of measurements of O_2 and CO_2 compositions. Coupling between the elemental balance (stoichiometric equations) and the macroscopic balance (gas balance, pH, conductivity, and pressure) allows to obtain an indirect measurement of the biomass activity and its concentration.[20]

This approach was used here. There are two gas components that are directly related to biomass activity in autotrophic conditions, which are respectively the oxygen which is produced and carbon dioxide which is consumed as a result of the microalgae photosynthetic growth.

These elements are bound by the following stoichiometric equation determined by elemental analysis of biomass:

$$CO_2 + 0.512H_2O + 0.0063SO_4^{2-} + 0.181NH_4^+ + 0.0213PO_4^{3-} \rightarrow CH_{1.77}O_{0.472}N_{0.181}S_{0.0063}P_{0.0213} + 1.0752O_2. \quad (17)$$

A mass balance on carbon dioxide consumed or on the oxygen produced can give a correct estimation of biomass concentration.[21]

Table 4. Experimental values of mass absorption coefficient E_a obtained under conditions of strict physical limitation in the PBR

I (µmole m^{-2} s^{-2})	110	300	500	1000
E_a (m^2 kg^{-1})	200	176	160	130

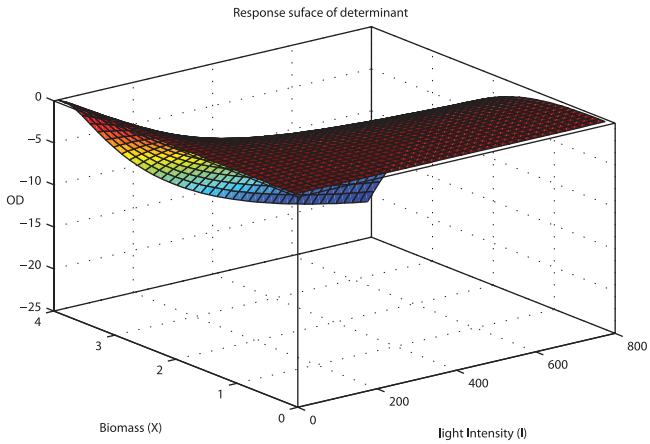

Figure 20. The response surface of the state space.

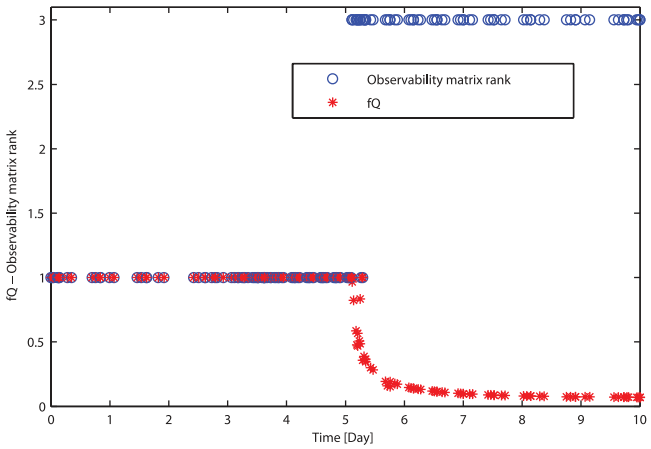

Figure 21. f_Q function and observability matrix rank.

Balance on oxygen

Oxygen is produced as a result of the photosynthetic growth of microalgae. Once produced, part of the O_2 is transferred into the gaseous phase. In the system under study, a gas vector N_2 is applied through the reactor. In these conditions, the accumulation of the dissolved oxygen into the liquid phase could be neglected; as a result, the produced oxygen rate (which is proportional to the growth rate) equals the oxygen transfer rate. A mass balance on O_2 into the gaseous phase allows determining on-line the oxygen production rate as the difference between inlet and outlet O_2 partial flow rates as follows:

$$Q_e C_{O_2,e} - Q_s C_{O_2,s} = QC_{O_2,p} \tag{18/}$$

where Q_e is the flow input, Q_s is the flow output, $C_{O_2,e}$ is the oxygen concentration at the input and $C_{O_2,s}$ is the oxygen concentration at output.

The oxygen production rate is correlated with the biomass growth rate by the stoichiometric coefficient of the equation:

$$QC_{O_2,p} = \frac{MX}{MO_2}\frac{1}{\vartheta O_2} \tag{19/}$$

where ϑ_{O_2} is the stoichiometric coefficient, which is equal to 1.075 mole of O_2/mole of biomass.

Balance on CO_2

The contribution of CO_2 is used to ensure the needs of the culture and to optimize biomass production. On the other hand, the CO_2 regulates the pH by controlled injection in the presence of a continuous bubbling of nitrogen to optimize culture conditions and avoid stressing the algae. The carbon balance is made by taking into consideration all forms of carbon produced, consumed or accumulated in the photobioreactor. It therefore relates to the injected carbon for pH control and carbon dioxide output of photobioreactor that has not been fixed by microalgae. We must also consider the total inorganic carbon (TIC) and total organic carbon (TOC) consumed or accumulated in the medium.

The pH is regulated every three hours. This is the time required for CO_2 that is not assimilated by the cells to exit entirely from the PBR. It is then easy to perform a balance on the input and output quantities. This balance gives the mass of carbon transferred (mCO_2) to the PBR, which a part can be assimilated by the cells, and the other part accumulated in the culture medium. One mole of CO_2 assimilated by the biomass leads to the production of one mole of biomass. The kinetics of growth is the result when the ratio of molar masses MC of carbon ($12\,g\,mol^{-1}$) and MX biomass ($24.72\,g\,mol^{-1}$).

$$QC_{CO_2,p}\frac{MX}{MC} = X_p. \tag{20/}$$

The four experiments, of which their operating conditions are presented in Table 3, were used to demonstrate the feasibility of determining the biomass produced from gas analysis. They were conducted in batches Figures 14 and 15 show: two in non-limited growth condition and two with sulphur limitation.

Balancing the carbon consumed and the oxygen produced can allow us to estimate the biomass concentration in the PBR from the balance presented above. As can be seen in Figures 23 and 24, the available data on oxygen and CO_2 reflect biomass production in both Growth experiments 1 and 2 rather well.

The balance of the carbon consumed and the oxygen produced in both Deprivation experiments 3 and 4 is shown in Figures 25 and 26. Note that the estimate of biomass from the balance of oxygen

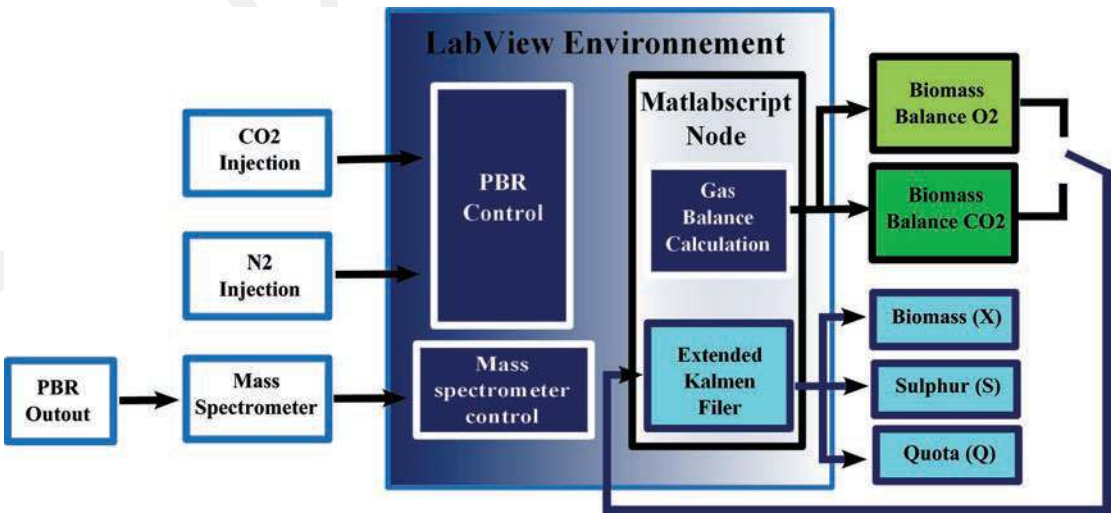

Figure 22. The program steps of the Extended Kalman Filter.

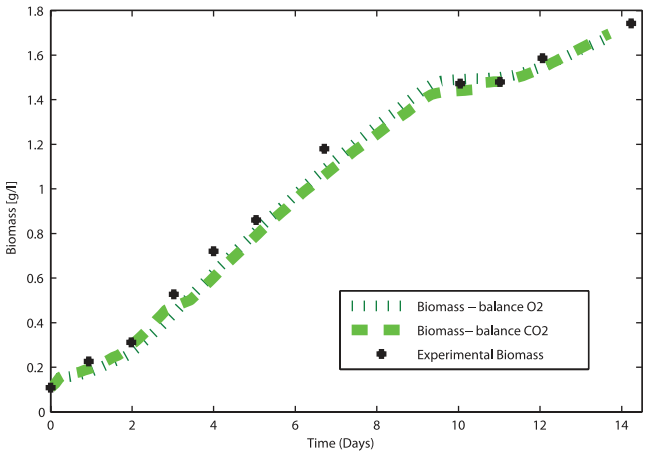

Figure 23. Evolution of biomass concentration, indirect measurements from O_2, CO_2 and dry matter—Growth experiment 1.

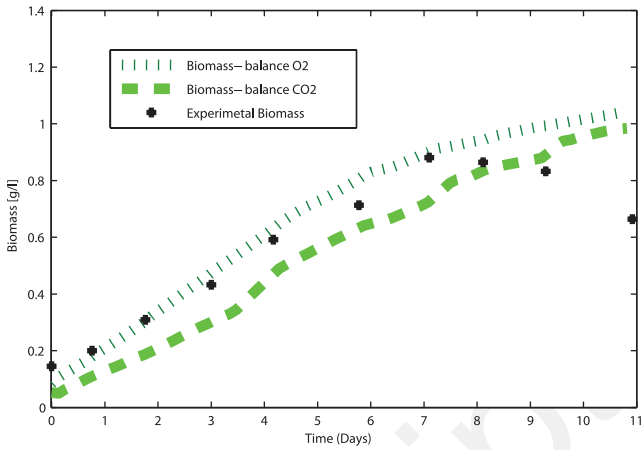

Figure 25. Evolution of biomass concentration, indirect measurements from O_2, CO_2 and dry matter—Deprivation experiment 3.

reflects biomass production rather well until the seventh day. Outside this zone, the decrease in biomass is not predicted correctly. From the available data on carbon, we find the same problem with a more limited reconstitution and significant differences. This is probably due to a change in reaction stoichiometry in the Sulphur deprivation phase and the production of secondary misidentified metabolites, which may be added as the accumulation of measurement errors. Signal drift of the mass spectrometer can cause a small error, but on a cumulative measure high frequency, this error becomes important.

EKF results using indirect measurement of the biomass concentration from O_2 and CO_2 by using Deprivation experiment 4 measurements

The choice of covariance matrix (R and Q) is important to estimate. The covariance matrix R corresponds to the measurements noise, assumed to be characterized here by a Gaussian noise. The system noise covariance matrix Q can be set based on the variance of the model uncertainty of each state. For the photobioreactor system, the values of Q and R were determined empirically, that is we repeated the simulation with new values of R and Q to find the best estimate. The best values obtained were $R = 10^4$ and $Q = \text{diag}\,[1, 10^{-3}, 10^{-3}]$. It was noted that when we have low values of R and important values of Q, the estimate is worse. This shows that we have an important measurement noise and that gives more confidence to the model. The covariance matrix Q was chosen in a diagonal form according to the usual assumption that the individual components (i.e., system noise vector) are uncorrelated.

Results of state estimation of the culture of *C. reinhardtii* with the Kalman filter via biomass estimated from the O_2 balance show a low convergence of the estimate (Figures 27 and 28). Indeed, the experiment starts in non-limiting conditions, thus in an unobservable configuration. It is reflected by a divergence of the filter at the beginning of experimentation. The system becomes observable when $f_Q < 1$ and the filter starts to converge.

Regarding extracellular concentrations of sulphur, we found the same problem in the simulation, that is a small divergence in the moment when $f_Q = 1$, then convergence until the end of the experiment (red line in Figure 27). Since there are no experimental data for the intracellular sulphur quota, we cannot compare them with the results of the filter. To verify that the divergence of the filter at the beginning of the experiment was due to the non-observability of the system, gain values were obtained when the filter has converged where it was used (blue line in Figure 27). It can be observed that the estimates improved.

We note that it is difficult to obtain a fast convergence also during deprivation phase for extracellular sulfate. The biomass (X) is not dependent on extracellular sulphur (S) directly, but on the

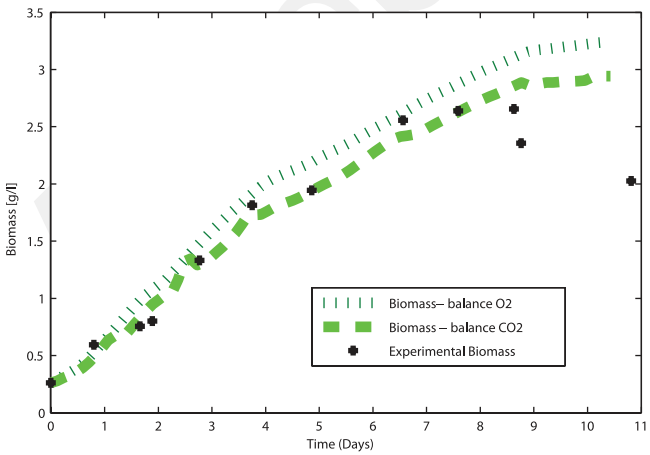

Figure 24. Evolution of biomass concentration, indirect measurements from O_2, CO_2 and dry matter—Growth experiment 2.

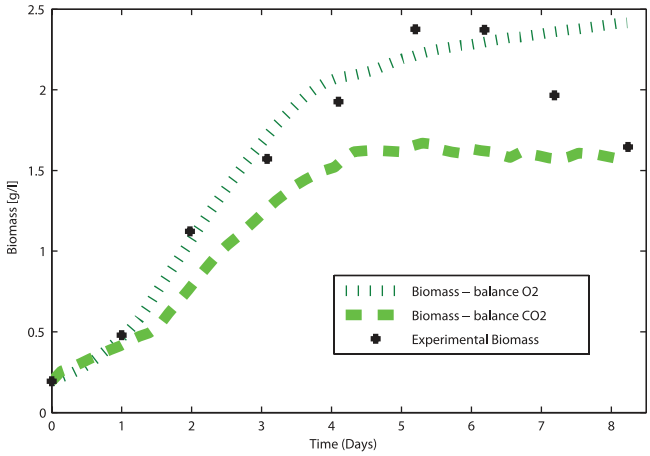

Figure 26. Evolution of biomass concentration, indirect measurements from O_2, CO_2 and dry matter—Deprivation experiment 4.

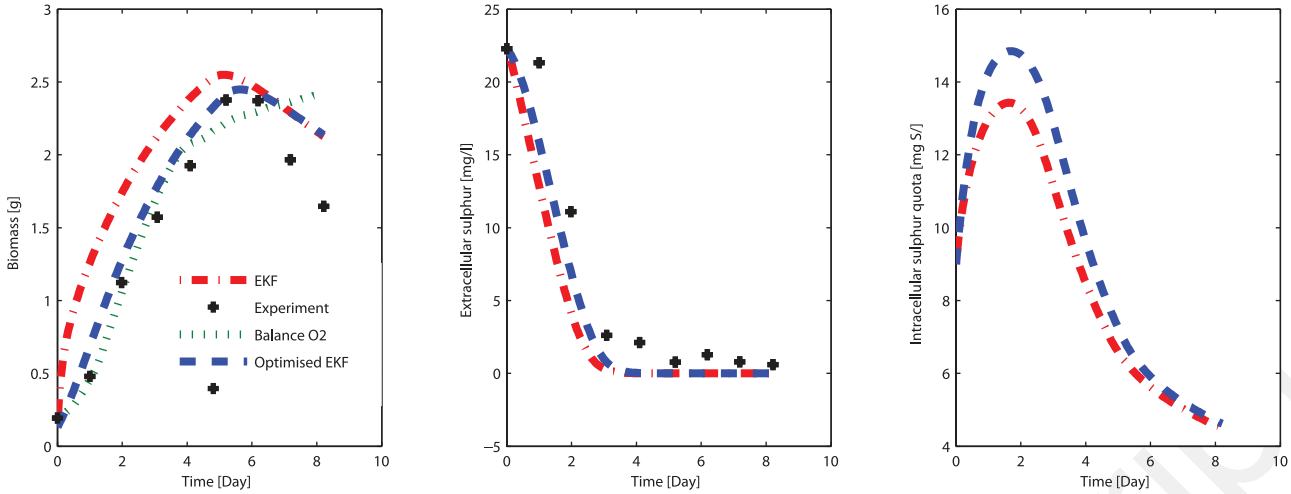

Figure 27. Evolution of biomass, extracellular sulphur concentration and intracellular sulphur quota concentration: estimation versus experimental data.

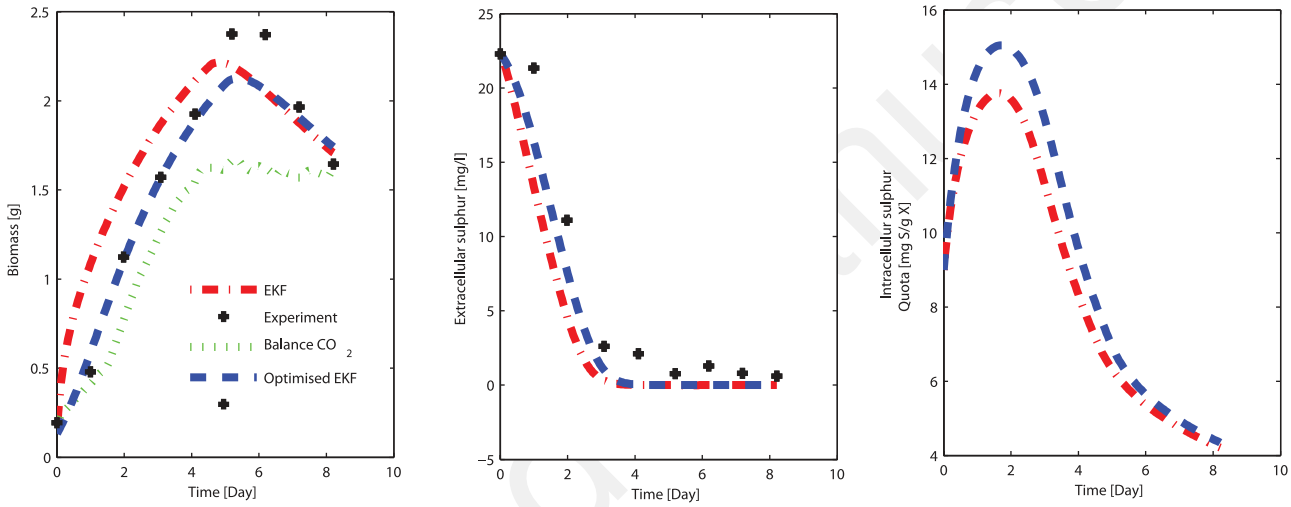

Figure 28. Evolution of biomass, extracellular sulphur concentration and intracellular sulphur quota concentration: estimation versus experimental data.

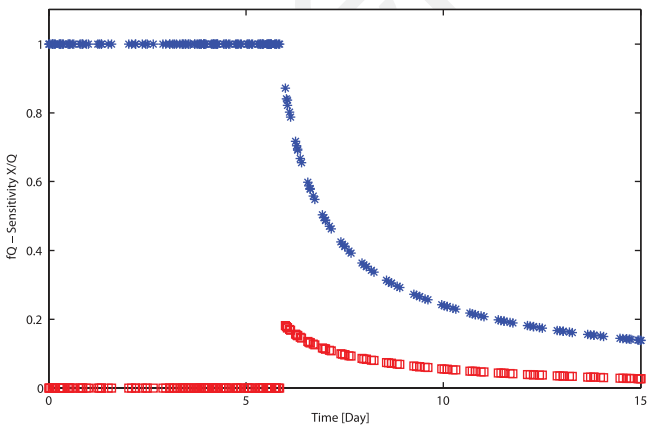

Figure 29. Simulation of the sensitivity function of X/Q (□) and f_Q function (*).

intracellular sulphur quota (Q), which itself depends on extracellular sulphur (S). The presence of the state variable $S = 22.28$ mg L^{-1} in the denominator in Equation (3), which is fairly large compared to $k_s = 3.7$, makes S little observable. In order to see the influence of the parameters relative to the other, a function of the sensitivity of the measurement (X/Q) has been plotted (Figure 29).

We also tested the filter on data from Deprivation experiment 3. The results are similar to those found in the Deprivation experiment 4 data.

CONCLUSION

A dynamic model of *Chlamydomonas reinhardtii* growth under light attenuation and sulphur-deprived conditions leading to hydrogen production in a photobioreactor is presented and a sensitivity analysis has been done. Sensitivity function analysis was revealed as an interesting tool to identify efficiently and accurately the parameters of the considered model. This analysis provided the most sensitive parameters for which special attention has to be paid during identification. Furthermore, it allowed us to

propose an identification procedure in three steps using measurements of biomass and extracellular sulphur concentrations collected with two different operating scenarios. Based on the shape of the sensitivity functions, time periods (in batch mode) were identified during which numerous measurements have to be collected for accurate parameter identification.

We found that the most sensitive parameters in the case non-limited growth are μ_{max}, K_I, and μ_s. The strong influence is in the same proportions on X, S, and Q. In turn, there is no influence of Y_{sx} and k_s parameters on X and poor influence on S. In the sulphur deprivation case, the sensitivity functions presented a maximum that corresponds to the moment when the internal sulphur quota reached its maximum. Furthermore, the parameters μ_{max}, K_I, and μ_s were also influential in sulphur deprivation phase. For the specific parameters of this case, the parameter f_{min} showed very little influence compared to the other two parameters, k and Q_m. k parameter has a maximum influence after two days of cultivation on X and S.

The second step consisted of the identification of the dominant parameters calculated in step one. This identification is the result of the minimization of the sum of squared deviations between experimental data and the corresponding simulated values. The identification of parameters allowed for a better prediction of the model and to overcome the uncertainties of the optical parameters. We note that the identification strategy developed has the advantage of giving a good approximation of parameters.

Balancing the carbon consumed and on the oxygen produced allowed us to estimate the biomass concentration in the PBR. The available data on oxygen and CO_2 reflect biomass production in both Growth experiments 1 and 2 rather well. For both Deprivation experiments 3 and 4, the estimation of biomass from the balance on oxygen reflects biomass production rather well until the seventh day. Outside this zone, the decrease in biomass is not predicted correctly. On available data on carbon, we find the same problem. So, a mass balance on carbon dioxide consumed and on the oxygen produced can give a correct estimation of biomass concentration.

Finally, the extended Kalman filter was chosen to estimate the three state variables X, S, and Q. We concluded that it provides a relevant response for the design of an extracellular sulphur concentration controller in limiting conditions inducing H_2 production. Even if the results are not entirely satisfactory because of the slow convergence of the filter, it still provides a relevant response for the design of an extracellular sulphur concentration controller in limiting conditions inducing H_2 production.

REFERENCES

[1] S. Fouchard, J. Pruvost, M. Titica, B. Degrenne, J. Legrand, *Biotechnol. Bioeng.* **2008**, *102*, 232.

[2] M. R. Droop, *J. Mar. Biol. Assoc. UK* **1968**, *48*, 689.

[3] O. Bernard, A. Sciandra, S. Madani, *Ecol. Modell.* **2007**, *211*, 324.

[4] L. Pottier, J. Pruvost, J. Deremetz, J. F. Cornet, J. Legrand, G. Dussap, *Biotechnol. Bioeng.* **2005**, *91*, 569.

[5] D. Dochain, *Bioprocess Control*, ISTE, London **2008**, p. 242.

[6] G. Bastin, D. Dochain, *On-Line Estimation and Adaptive Control of Bioreactors*, Elsevier, Amsterdam **1990**, p. 379.

[7] J. Mailier, A. Delmontte, M. Cloutier, M. Jolicoeur, A. Vande Wouwer, *Biotechnol. Bioeng.* **2011**, *108*, 5.

[8] E. Walter, L. Pronzato, *Identification of Parametric Models From Experimental Data*, Springer-Verlag, Berlin **1997**, p. 413.

[9] G. Becerra-Celis, S. Tebbani, C. Joannis-Cassan, A. Isambert, P. Boucher, "Estimation of microalgal photobioreactor production based on total inorganic carbon in the medium," *IFAC Proceedings of the 17th World Congress: The International Federation of Automatic Control*, **2008**, p. 14582.

[10] L. Jian, N. S. Xu, W. W. Su, *Biochem. Eng. J.* **2003**, *14*, 65.

[11] G. A. Ifrim, M. Titica, M. Barbu, L. Boilereaux, G. Cogne, S. Carman, J. Legrand, *Chem. Eng. J.* **2013**, *218*, 191.

[12] J. F. Cornet, G. Dussap, *Biotechnol. Prog.* **2009**, *25*, 424.

[13] I. Smets, K. Bernaerts, J. Sun, K. Marchal, J. Vanderleyden, J. Van Impe, *Biotechnol. Bioeng.* **2002**, *80*, 195.

[14] Y. C. Huang, H. D. Yeh, *J. Hydrol.* **2007**, *335*, 406.

[15] A. H. Jazwinski, *Stochastic Processes and Filtering Theory*, New York Academic, New York **1970**, p. 376.

[16] D. G. Luenberger, *Optimization by Vector Space Methods*, Wiley—Interscience, New York **1969**, p. 326.

[17] B. Degrenne, J. Pruvost, G. Christophe, J. F. Cornet, G. Cogne, J. Legrand, *Int. J. Hydrogen Energy* **2010**, *35*, 10741.

[18] B. Degrenne, J. Pruvost, J. Legrand, *Bioresour. Technol.* **2011**, *102*, 1035.

[19] H. Takache, G. Christophe, J. F. Cornet, J. Pruvost, *Biotechnol. Prog.* **2010**, *26*, 431.

[20] J. E. Claes, J. F. Van Impe, *Bioprocess Eng.* **2000**, *22*, 195.

[21] S. Fouchard, J. Pruvost, B. Degrenne, M. Titica, J. Legrand, *Int. J. Hydrogen Energy* **2008**, *33*, 3302.